Hunan Daxue Xuebao/Journal of Hunan University Natural Sciences
ISSN : 1674-2974 | CN 43-1061 / N

DOI: 10.5281/zenodo.15166760
Vol: 62 | Issue: 04 | 2025

FLUID STRUCTURE INTERACTION FOR STRESS COMPUTATION OF CONVENTIONAL AND COMPOSITE MATERIAL JOURNAL BEARING

B. MADHAVI*
Assistant Professor, Department of Mechanical Engineering, ICFAI Foundation for Higher Education-IFHE, Hyderabad, India. *Corresponding Author

M.L. PAVAN KISHORE
Assistant Professor, Department of Mechanical Engineering, ICFAI Foundation for Higher Education-IFHE, Hyderabad, India. Email: kishoreml@ifheindia.org

PRIYANKA CHATTORAJ
Assistant Professor, Department of Mechanical Engineering, ICFAI Foundation for Higher Education-IFHE, Hyderabad, India.

Abstract

In modern industrial manufacturing, fluid film journal bearings play a critical role in supporting high-speed rotating equipment subjected to significant rotor loads. This study presents a novel numerical approach for predicting stress distribution in journal bearings using fluid-structure interaction (FSI) simulations conducted with ANSYS Fluent software. Journal bearings, a critical component in rotating machinery, experience complex interactions between the lubricant flow and the structural components, which can lead to significant stress concentrations. The study employs a coupled computational approach combining fluid dynamics and structural mechanics to simulate the behavior of the journal bearing under various operating conditions. The fluid flow is modeled using the Navier-Stokes equations, while the structural deformation is analyzed through elasticity theory. The FSI method captures the dynamic interplay between the lubricant pressure distribution and the induced stresses in the bearing material. By conducting simulations over a range of different L/D ratios (0.5, 1.0, and 1.5) and eccentricity ratios (0.3, 0.5, 0.7, and 0.9) the study provides valuable insights into stress distribution patterns, particularly at critical locations such as the bearing surface and housing. The results offer a predictive framework for enhancing the design and durability of journal bearings, contributing to improved reliability in engineering applications.

Keywords: *Deformation, Eccentricity Ratio, J-Integral, L/D Ratio, Stress Intensity Factors (SIFS).*

1. INTRODUCTION

Journal bearings, crucial in many mechanical systems, undergo complex interactions between the lubricating fluid and the solid structure. Understanding the stress distribution within these bearings is critical for improving their performance and reliability. Fluid-Structure Interaction (FSI) has emerged as a powerful tool for predicting stress distribution by accounting for the interplay between fluid dynamics and structural deformations. Heshmat et al. [1] (2000) presented one of the early attempts to incorporate fluid-structure interaction in journal bearing analysis, focusing on gas-lubricated foil bearings. Their study introduced a numerical model that coupled the Reynolds equation with a simple structural model for compliant foil bearings. The authors demonstrated the importance of considering structural deformation in predicting bearing performance, particularly for high-speed applications. While their model was limited in its ability to capture complex stress distributions, it laid the groundwork for future FSI studies in journal bearings. Gadangi and Palazzolo [2] (2000) developed a finite element model for the analysis of fluid film journal bearings, incorporating both thermal and

DOI: 10.5281/zenodo.15166760
Vol: 62 | Issue: 04 | 2025

elastic deformation effects. Their work utilized a transient analysis approach, considering pad flexibility and fluid film temperature variations. The study highlighted the significance of considering multi physics phenomena in journal bearing analysis, particularly for predicting accurate stress distributions. Their model provided insights into the dynamic behavior of tilt pad journal bearings under various operating conditions. Lahmar et al. [3] (2002) introduced a thermos-hydrodynamic analysis of a dynamically loaded journal bearing. Their model considered both thermal and elastic deformation effects, using a finite difference method to solve the generalized Reynolds equation. The study revealed the significant impact of thermal effects on bearing performance and stress distribution, particularly under dynamic loading conditions. Their work emphasized the need for comprehensive models that account for multiple physical phenomena in journal bearing analysis. Boncompain et.al.[4] (2003) presented a comprehensive model for journal bearing analysis, incorporating both thermal and elastic deformation effects. Their approach used a finite difference method to solve the Reynolds equation coupled with a finite element model for the bearing structure. The study highlighted the significant impact of thermal effects on bearing performance and stress distribution. Although the fluid-structure coupling was not fully two-way, their work emphasized the need for multi physics approaches in accurate journal bearing analysis.

Bouyer and Fillon [5] (2004) conducted experimental studies on the thermal behaviour of journal bearings, providing valuable data for validating numerical models. Their work focused on measuring friction torque during start-up conditions, revealing the complex interactions between thermal effects and bearing performance. The experimental results highlighted the importance of considering transient thermal behaviour in stress analysis of journal bearings. This study provided crucial benchmark data for the development and validation of numerical FSI models. Kucinschi et al. [6] (2006) made significant strides in FSI modelling of journal bearings by introducing a fully coupled thermos-elasto hydrodynamic (TEHD) model. Their approach utilized a finite element method for both fluid and structural domains, allowing for more accurate prediction of stress distributions. The authors demonstrated how thermal expansion and elastic deformation could significantly alter the pressure distribution and load-carrying capacity of the bearing. This work was instrumental in showcasing the importance of considering multiple physical phenomena in journal bearing analysis. Suh and Chae [7] (2007) developed a mixed elasto hydrodynamic lubrication model for journal bearings, considering surface roughness effects. Their work combined Reynolds equation with elastic deformation and surface roughness models to provide a more realistic representation of bearing behavior. The study revealed how micro-scale surface features influence pressure distribution and, consequently, stress patterns in the bearing. Their findings emphasized the importance of considering surface topography in accurate stress prediction for journal bearings.

Wang et.al.[8] (2009) focused on the dynamic behaviour of journal bearings using an FSI approach. They developed a time-dependent model that coupled the Reynolds equation with a structural dynamics model. The study revealed how fluid-structure interaction affects the stability and vibration characteristics of journal bearings under various operating conditions. Their work was particularly valuable in understanding the transient behaviour of bearings during start-up and shutdown processes, providing insights into stress variations during these critical phases. Bouchoule et al. [9] (2010) presented a numerical study on the influence of thermal effects on the dynamic behaviour of rotor-bearing systems in cryogenic turbopumps. Their work combined a thermal model with dynamic analysis to predict bearing performance under extreme temperature conditions. The study highlighted the unique challenges of modelling journal bearings in cryogenic environments and the significant impact of thermal gradients on stress distributions. Their findings provided valuable insights for the design of bearings in specialized applications such as aerospace propulsion systems. Liang et al. [10] (2012) introduced a novel approach to FSI modelling in journal bearings by incorporating cavitation

DOI: 10.5281/zenodo.15166760
Vol: 62 | Issue: 04 | 2025

effects. Their model used a mass-conserving algorithm for cavitation treatment coupled with an elastic deformation model for the bearing structure. The study demonstrated how cavitation could significantly affect the pressure distribution and, consequently, the stress patterns in the bearing. This work was crucial in improving the accuracy of stress predictions in journal bearings operating under cavitating conditions. Dousti et al. [11] (2013) developed a thermos-hydrodynamic model for journal bearings operating under turbulent flow conditions. Their work expanded the understanding of stress distributions in high-speed bearings by incorporating inertial effects in both temporal and convective terms. The study revealed how turbulence influences pressure distribution and heat generation in journal bearings. Their findings were particularly relevant for predicting stress patterns in bearings operating at high Reynolds numbers, common in many industrial applications. Brito et al. [12] (2015) presented a comprehensive FSI model for journal bearings that included both thermal and cavitation effects. Their approach used a finite volume method for the fluid domain and a finite element method for the structural domain, with a robust coupling algorithm. The authors conducted extensive parametric studies to investigate the effects of various operational and design parameters on bearing performance and stress distribution.

This work provided valuable insights into optimizing journal bearing designs for different applications. Jiang et al. [13] (2016) investigated the effects of surface texturing on the performance of journal bearings using a multi physics approach. Their model incorporated thermal effects, cavitation, and elastic deformation to provide a comprehensive analysis of textured bearings. The study revealed how strategically designed surface textures could alter pressure distributions and reduce friction, thereby influencing stress patterns in the bearing. Their work opened new avenues for enhancing journal bearing performance through surface engineering. Zhang et al. [14] (2018) focused on developing a more efficient FSI algorithm for journal bearing analysis. They introduced a novel partitioned coupling scheme that significantly reduced computational time while maintaining accuracy. The study included a detailed comparison of different coupling strategies and their impact on predicting stress distributions. Their work was particularly valuable for enabling more complex parametric studies and optimization processes in journal bearing design. Alakhramsing et al. [15] (2019) presented a model for elasto-hydrodynamic lubrication of journal bearings under severe operating conditions. Their work introduced a new mass-conserving cavitation algorithm coupled with thermal and elastic deformation models. The study provided insights into stress distributions under extreme loading scenarios, particularly focusing on the transition between fully-flooded and starved lubrication regimes. Their findings were crucial for predicting bearing behaviour and stress patterns in demanding industrial applications. Wang et al. [16] (2020) developed a multiscale model for journal bearings, considering both macro-scale fluid dynamics and micro-scale surface interactions. Their approach combined computational fluid dynamics with a homogenized Reynolds equation to capture the effects of surface roughness and texturing.

The study provided a more comprehensive understanding of stress generation mechanisms, revealing how micro-scale features influence macro-scale bearing performance. This work represented a significant step towards more realistic modelling of journal bearing behaviour. Kumar et al. [17] (2021) expanded the FSI analysis of journal bearings to include surface texture effects. Their model incorporated micro-scale surface features into the fluid-structure interaction, revealing how these textures influence pressure distribution and stress patterns. The study demonstrated that properly designed surface textures could reduce friction and wear while altering the stress distribution in the bearing. This work opened new avenues for enhancing journal bearing performance through surface engineering. Li et al. [18] (2021) investigated the impact of non-Newtonian lubricants on journal bearing performance using an FSI approach. Their model incorporated shear-thinning and viscoelastic fluid behaviour into the traditional elasto-hydrodynamic framework. The study revealed how complex

DOI: 10.5281/zenodo.15166760
Vol: 62 | Issue: 04 | 2025

fluid rheology affects pressure distribution and film thickness, consequently influencing stress patterns in the bearing. Their findings provided valuable insights for the design of bearings using advanced lubricants in specialized applications. Zhao et al. [19] (2022) developed a machine learning-enhanced model for rapid prediction of journal bearing performance. Their approach combined proper orthogonal decomposition with artificial neural networks to create an efficient surrogate model. While not directly focused on stress analysis, their work paved the way for more efficient computational methods in bearing design and optimization. The rapid prediction capabilities offered by their model could potentially be extended to stress analysis, enabling real-time monitoring and predictive maintenance strategies. Chen et al. [20] (2022) presented a comprehensive review of recent advancements in journal bearing modelling, including FSI approaches. Their work provided a valuable overview of the state-of-the-art in numerical methods for bearing analysis, covering topics such as multi physics coupling, surface texturing, and advanced lubricant models. The review highlighted emerging trends in journal bearing research and identified key challenges in accurately predicting stress distributions.

This work serves as an essential reference for researchers and engineers in the field of journal bearing analysis. Patel and Deheri [21] (2023) investigated the effects of magnetic fields on the performance of journal bearings using an FSI approach. Their model incorporated magneto hydrodynamic effects into the traditional Reynolds equation, coupled with elastic deformation analysis. The study revealed how magnetic fields could be used to control pressure distribution and film thickness, thereby influencing stress patterns in the bearing. Their work expanded the understanding of stress distributions in bearings operating under electromagnetic influences, opening new possibilities for active control of bearing performance. Zhang et.al.[22] (2023) developed a novel FSI model incorporating wear prediction for journal bearings. Their approach coupled fluid dynamics, structural mechanics, and a wear model to simulate the long-term evolution of bearing geometry and performance. The study demonstrated how wear processes influence stress distributions over time, providing insights into the lifecycle behaviour of journal bearings. This work represented a significant advancement in predicting the long-term reliability and maintenance requirements of journal bearings in industrial applications. Liu et al. [23] (2023) presented a GPU-accelerated FSI model for journal bearings, significantly reducing computation time for complex simulations. Their approach leveraged parallel computing techniques to solve the coupled fluid-structure equations efficiently. The study showcased how advanced computational methods could enable more detailed parametric studies of stress distributions in journal bearings. This advancement in computational efficiency opened new possibilities for real-time analysis and optimization of bearing designs.

Meruane et.al.[24] (2024) introduced a digital twin concept for journal bearings, integrating real-time data with FSI models for predictive maintenance. Their approach combined sensor data with a physics-based model to provide continuous monitoring of bearing performance and stress states. The study demonstrated how digital twin technology could enable proactive maintenance strategies, potentially reducing downtime and extending bearing life. This work represented a significant step towards the integration of advanced numerical models with industrial Internet of Things (IoT) systems. Chen et al. [25] (2024) presented recent advancements in FSI modelling for journal bearings, incorporating machine learning techniques to enhance computational efficiency. Their approach used neural networks to predict fluid behaviour, which was then coupled with a traditional FEA model for structural analysis. The study demonstrated how this hybrid approach could significantly reduce computation time while maintaining high accuracy in stress predictions. This work represents the cutting edge of numerical methods for journal bearing analysis, potentially enabling real-time stress monitoring and predictive maintenance strategies. Wang et al. [26] (2024) developed a multi physics model for journal bearings in extreme environments, considering radiation effects alongside

DOI: 10.5281/zenodo.15166760
Vol: 62 | Issue: 04 | 2025

traditional FSI phenomena. Their work expanded the application of stress analysis to specialized bearing applications in nuclear and space industries. The study revealed how radiation-induced material changes could affect bearing performance and stress distributions over time. This research provided crucial insights for the design and maintenance of bearings in high-radiation environments, addressing a previously understudied aspect of journal bearing analysis. Kango et al. [27] (2024) presented a novel approach to modelling journal bearings with smart materials, incorporating piezoelectric effects into the FSI framework. Their study explored how active control of bearing surfaces could be used to optimize performance and reduce stress concentrations. The model coupled electromagnetic fields with fluid dynamics and structural mechanics to provide a comprehensive analysis of smart bearing behaviour. This work opened new avenues for adaptive bearing designs capable of responding to changing operational conditions. Zhu et.al.[28] (2024) developed an advanced FSI model for journal bearings operating with nano lubricants.

Their approach incorporated nanoparticle distribution and its effects on fluid properties into the traditional elasto hydrodynamic framework. The study revealed how nanoparticles influence pressure distribution, film thickness, and consequently, stress patterns in the bearing. This research provided valuable insights into the potential benefits and challenges of using nano lubricants in high-performance journal bearing applications. Lebon et.al.[29] (2024) presented a multiscale FSI model for journal bearings with functionally graded materials (FGMs). Their approach combined homogenization techniques with traditional FSI analysis to capture the effects of spatially varying material properties on bearing performance. The study demonstrated how strategically designed FGMs could optimize stress distributions and enhance bearing durability. This work represented a significant advancement in tailoring bearing materials for specific operational requirements. Tauviqirrahman et al. [30] (2024) investigated the effects of slip boundary conditions on journal bearing performance using an advanced FSI model. Their study incorporated slip flow models into the Reynolds equation, coupled with elastic deformation analysis. The research revealed how engineered slip surfaces could alter pressure distributions and reduce friction, thereby influencing stress patterns in the bearing. This work provided new insights into the design of low-friction bearings for energy-efficient applications.

2. PROBLEM STATEMENT

In modern industrial manufacturing, high-speed rotating equipment is subjected to heavy rotor loads, requiring robust and efficient fluid film journal bearings to ensure smooth operation and long-term reliability. The primary challenge lies in accurately predicting the performance of these bearings, especially under varying load and speed conditions. Fluid film journal bearings must withstand substantial loads while facilitating relative motion between the rotating journal and the bearing surface, relying on a fluid film to reduce friction and wear. However, predicting the behavior of the fluid film and the resulting stresses on the bearing surfaces remains complex, especially when considering various design parameters such as eccentricity ratios and L/D ratios. The need for reliable prediction of bearing performance under different operational conditions, while minimizing wear and optimizing load-carrying capacity, is a key problem in high-performance bearing design. In this part of the research work the stress and deformation determination of Journal Bearing is carried out for varying L/D ratios (0.5, 1.0, and 1.5) and eccentricity ratios (0.3, 0.5, 0.7, and 0.9).

3. METHODOLOGY

To address this problem, three-dimensional simulations were conducted using the ANSYS Fluent software package, which provides robust tools for fluid-structure interaction and turbulence modeling. The methodology involves simulating the journal bearing's behavior under various

DOI: 10.5281/zenodo.15166760
Vol: 62 | Issue: 04 | 2025

turbulent models to determine their efficiency and accuracy in stress and load prediction. Key design parameters—such as static strain, wall shear stress, and load-carrying capacity—are considered. The analysis focuses on different L/D ratios (0.5, 1.0, 1.5) and eccentricity ratios (0.3, 0.5, 0.7, 0.9) to understand their effects on bearing performance depicted in Table 1. By comparing the results across different models and design configurations, this approach allows for a comprehensive understanding of how varying geometric and operational parameters influence the stress distribution, fluid flow, and overall performance of the fluid film journal bearing system.

Table 1: Specification of Journal Bearing

L/D Ratio	Eccentricity Ratio			
0.5	0.3	0.5	0.7	0.9
1.0	0.3	0.5	0.7	0.9
1.5	0.3	0.5	0.7	0.9

4. MATERIALS AND METHODS

4.1. Babbit Material as Base line Material:

Babbitt material has been a traditional choice for bearing applications due to its outstanding tribological properties. The density of 2700 kg/m³ provides an optimal balance of support and conformability, which helps in forming a consistent oil film during operation. The material's softness allows it to embed any dirt particles that might enter the bearing system, protecting the shaft from damage. The relatively low hardness also means it can conform to minor shaft misalignments during initial running-in periods, creating an ideal bearing surface profile.

4.2. Carbon Epoxy as a bearing material:

Carbon Epoxy represents a modern evolution in bearing technology, with its advanced fiber-reinforced structure providing exceptional strength in the primary load direction through its high elastic modulus of 142 GPa. The material's low density of 1600 kg/m³ significantly reduces centrifugal forces and inertial loads, making it particularly advantageous for high-speed rotating equipment and aerospace applications. The distinct difference between longitudinal (E_x = 142 GPa) and transverse (E_y = 10 GPa) elastic moduli demonstrates the material's engineered anisotropic properties, allowing designers to optimize load-bearing capabilities in specific directions. The moderate Poisson's ratios (γ_{xy} = 0.16, γ_{yz} = 0.2) indicate the material's ability to maintain dimensional stability under varying load conditions, which is crucial for maintaining proper bearing clearances during operation. The shear modulus values (G_{xy} = 5.2 GPa, G_{yz} = 3.8 GPa) ensure adequate resistance to deformation under tangential loads, preserving bearing geometry during dynamic loading conditions. These properties combined make Carbon Epoxy an excellent choice for advanced bearing applications where traditional metallic materials may fall short, particularly in environments demanding high performance with minimal weight penalties.

The material properties of both conventional material and Carbon epoxy are depicted in corresponding Tables 2 and Table3.

Table 2: Properties of Babbitt Material

Properties	Material (Aluminium Alloy)
Young's modulus	53 GPa
Poisson's ratio	0.35
Shear Modulus	20GPa
Density	2700 Kg/m^3

Hunan Daxue Xuebao/Journal of Hunan University Natural Sciences
ISSN：1674-2974 | CN 43-1061 / N

DOI: 10.5281/zenodo.15166760
Vol: 62 | Issue: 04 | 2025

Table 3: Properties of Carbon Epoxy Material

Material	E_x(GPa)	E_y(GPa)	γ_{xy}	γ_{yz}	G_{xy}(GPa)	G_{yz}(GPa)	Density(g/cc)
Carbon Epoxy	142	10	0.16	0.2	5.2	3.8	1600

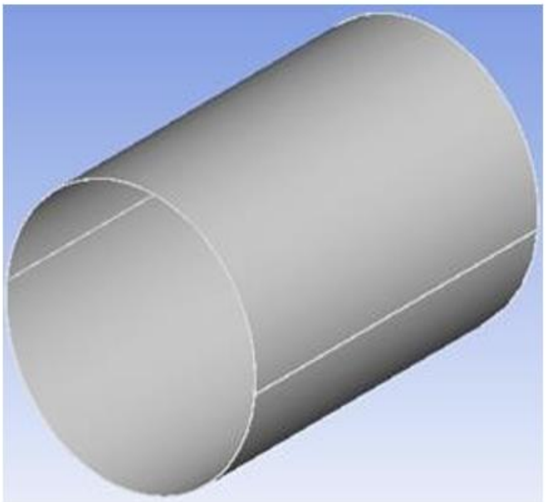

Figure 1:Three-dimensional Model of Bearing

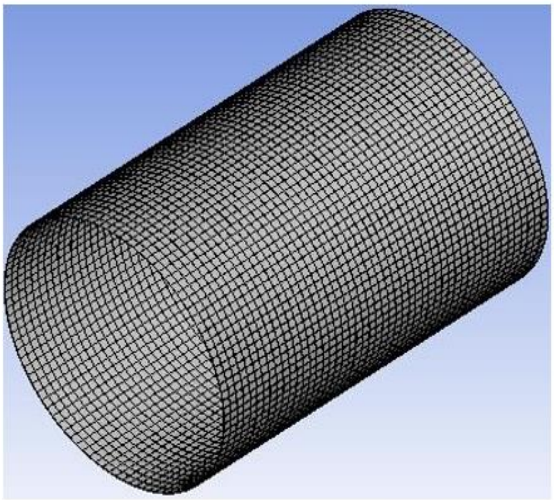

Figure 2: Meshed Model of Bearing

5. NUMERICAL MODELLING

Fluid-structure interaction (FSI) analysis for journal bearings combines computational fluid dynamics (CFD) and finite element analysis (FEA) to accurately predict bearing performance and stress distribution. The process typically begins with creating a detailed 3D model of the journal bearing in SolidWorks, including the shaft, bearing, and fluid domain Figure 1. This model is then imported into ANSYS Workbench for FSI simulation. The CFD component analyzes the fluid flow and pressure distribution within the bearing clearance, while the FEA component calculates the resulting stresses and deformations in the bearing structure. ANSYS Workbench's two-way coupling capability allows for iterative data exchange between the fluid and structural solvers, capturing the complex interactions between the lubricant flow and bearing deformation. This approach provides more accurate stress predictions compared to traditional methods, accounting for factors such as pressure-induced deformation and its effect on fluid film thickness.

6. FINITE ELEMENT METHOD

In the present computational fluid dynamics study, a distinct mesh structures to accurately model both smooth and dimpled rotor-stator configurations is developed shown in the Figure 2. The smooth setup, encompassing both single and dual geometry’s, employed a grid composed of 6,576 hexahedral elements. This mesh design proved suitable for capturing the flow characteristics in the absence of surface features. For the dimpled rotor-stator model, a more intricate mesh structure consisting of 3,344 hexahedral elements is crafted.

The reduction in overall element count, however, does not indicate a less detailed model. On the contrary, a highly refined mesh within and around the dimple regions to precisely capture the complex flow dynamics at these critical points are implemented. The decision to use a finer mesh for the dimpled areas stems from the need to accurately resolve the steep gradients occurring at the inlet and outlet sections of each dimple. These regions are prone to rapid changes in fluid behaviour, necessitating higher resolution to ensure computational accuracy. Despite the localized refinement,

DOI: 10.5281/zenodo.15166760
Vol: 62 | Issue: 04 | 2025

the overall element count for the dimpled model remains lower than its smooth counterpart. This apparent paradox is a result of our targeted approach to mesh refinement, focusing computational resources where they are most needed. This tailored approach to mesh design allows us to balance computational efficiency with accuracy, ensuring that our simulations capture the essential fluid dynamics within the rotor-stator system while optimizing resource utilization.

7. RESULTS AND OBSERVATIONS

The presented data offers a comprehensive analysis of Fluid-Structure Interaction (FSI) in journal bearings, examining the effects of varying L/D ratios and eccentricity ratios on key performance parameters. The study encompasses three different L/D ratios (0.5, 1.0, and 1.5) and four eccentricity ratios (0.3, 0.5, 0.7, and 0.9) for each L/D configuration. The results provide insights into pressure distribution, displacement, stress, and safety factors across these configurations Figure 3 to Figure 6. Additionally, the analysis extends to fracture mechanics parameters, specifically the J-integral and Stress Intensity Factors (SIFs), which are crucial for assessing the bearing's structural integrity under various operating conditions

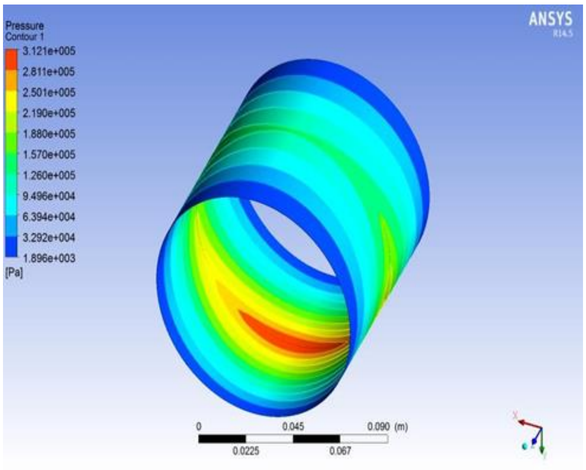

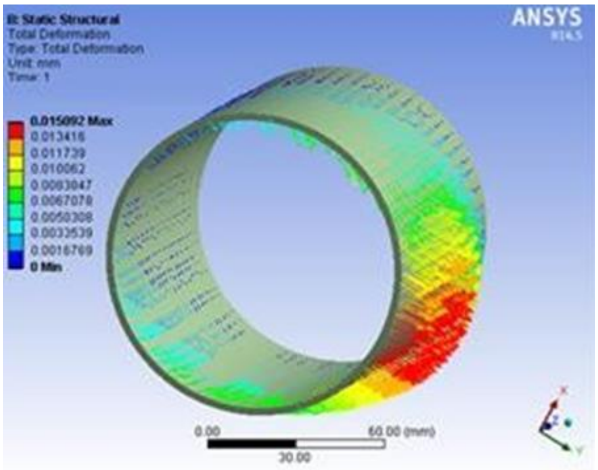

Figure 3: Pressure contour plot Figure 4: Total Deformation plot

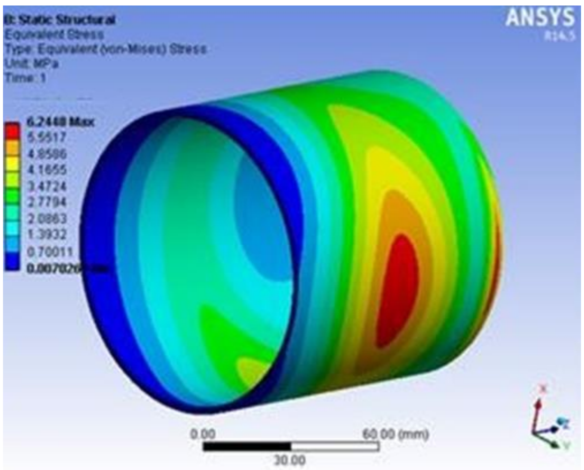

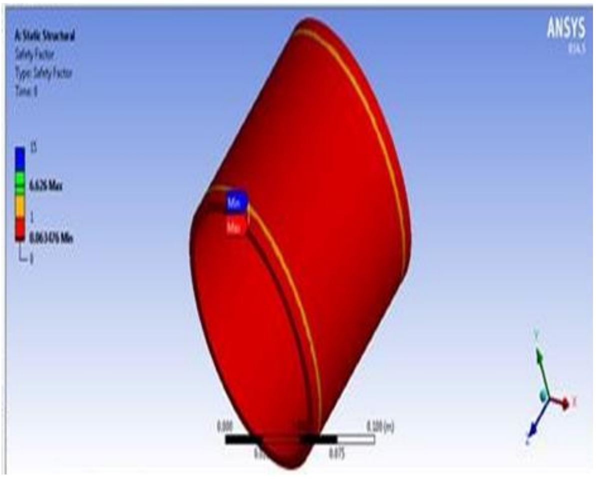

Figure 5: Equivalent Stress plot Figure 6: Safety Factor Contour plot

Hunan Daxue Xuebao/Journal of Hunan University Natural Sciences
ISSN：1674-2974 | CN 43-1061 / N

DOI: 10.5281/zenodo.15166760
Vol: 62 | Issue: 04 | 2025

Table 4: FSI Results for L/D ratio=0.5

L/D ratio	Eccentricity ratio	Pressure (Pa)	Displacement (mm)	Stress (MPa)	Safety factor
0.5	0.3	1.49E+05	0.0029644	2.7608	2.8808
	0.5	2.066E+05	0.0053614	3.8927	2.0471
	0.7	2.812E+05	0.0083703	6.1225	1.504
	0.9	3.634E+05	0.010352	7.5886	1.1638

Table 5: FSI Results for L/D ratio=1.0

L/D ratio	Eccentricity ratio	Pressure (Pa)	Displacement (mm)	Stress (MPa)	Safety factor
1.0	0.3	2.488E+05	0.0086261	4.8936	8.3118
	0.5	3.121E+05	0.015092	6.2448	6.626
	0.7	4.031E+05	0.026131	10.581	5.0137
	0.9	5.379E+05	0.045613	16.994	3.7572

Table 6: FSI Results for L/D ratio=1.5

L/D ratio	Eccentricity ratio	Pressure (Pa)	Displacement (mm)	Stress (MPa)	Safety factor
1.5	0.3	3.523E+05	0.019325	7.0022	5.6082
	0.5	4.215E+05	0.041523	10.241	4.6875
	0.7	5.151E+05	0.07221	16.498	3.8357
	0.9	6.449E+05	0.10981	23.94	3.0637

The results plotted in the Table 4 to Table 6 for varying L/D ratios (0.5, 1.0, and 1.5), a comprehensive overview of the results and the trends observed across these configurations.

1. For the L/D ratio of 0.5, which represents a relatively short bearing, we see the lowest overall values for pressure, displacement, and stress across all eccentricity ratios. As the eccentricity ratio increases from 0.3 to 0.9, we observe a steady increase in all parameters. The pressure rises from 1.49E+05 Pa to 3.634E+05 Pa, displacement increases from 0.0029644 mm to 0.010352 mm, and stress escalates from 2.7608 MPa to 7.5886 MPa. Conversely, the safety factor decreases from 2.8808 to 1.1638 as eccentricity increases.

2. Moving to the L/D ratio of 1.0, which represents a square aspect ratio bearing, we see higher values for all parameters compared to the 0.5 ratio. Pressure ranges from 2.488E+05 Pa to 5.379E+05 Pa, displacement from 0.0086261 mm to 0.045613 mm, and stress from 4.8936 MPa to 16.994 MPa as eccentricity increases. The safety factors are generally higher than in the 0.5 ratio case, ranging from 8.3118 to 3.7572.

3. For the L/D ratio of 1.5, representing a longer bearing, we observe the highest values for pressure, displacement, and stress. Pressure increases from 3.523E+05 Pa to 6.449E+05 Pa, displacement from 0.019325 mm to 0.10981 mm, and stress from 7.0022 MPa to 23.94 MPa across the eccentricity range. Safety factors are lower than in the 1.0 ratio case but higher than in the 0.5 ratio case, decreasing from 5.6082 to 3.0637 as eccentricity increases.

These trends can be explained by several factors:

1. Increased bearing length (higher L/D ratio) provides a larger surface area for pressure distribution, resulting in higher overall pressures and consequently higher stresses and displacements.

2. Longer bearings (higher L/D ratios) are more susceptible to bending and deformation, which explains the higher displacement values.

ISSN：1674-2974 | CN 43-1061 / N

DOI: 10.5281/zenodo.15166760
Vol: 62 | Issue: 04 | 2025

3. The higher pressures in longer bearings lead to increased stress concentrations, particularly at high eccentricity ratios.
4. The non-linear increase in parameters with eccentricity is due to the reduced fluid film thickness at higher eccentricities, leading to more pronounced hydrodynamic effects.
5. The intermediate L/D ratio of 1.0 shows the best safety factors, suggesting an optimal balance between load-bearing capacity and stress distribution. The shorter bearing (0.5 ratio) may not distribute the load as effectively, while the longer bearing (1.5 ratio) experiences higher bending stresses.

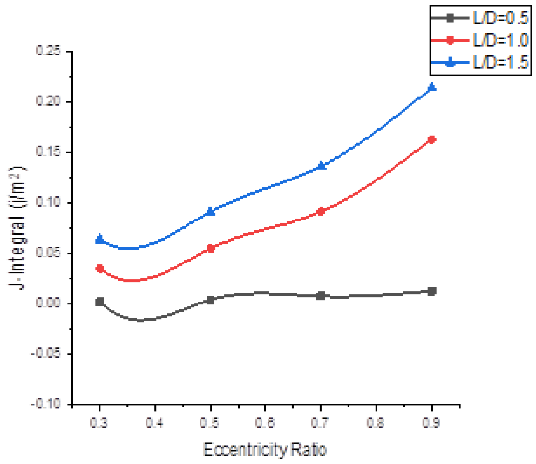

Figure 7: J-integral vs Eccentricity Ratio

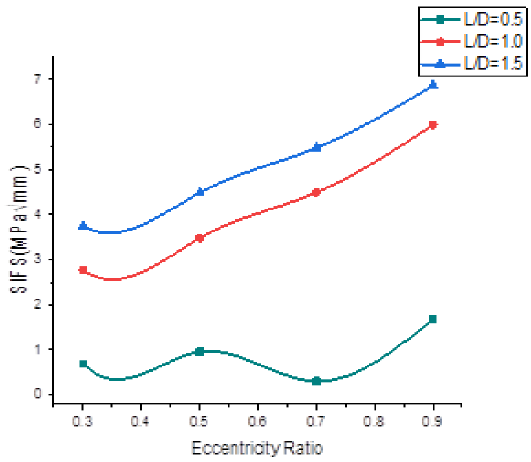

Figure 8: SIFS vs Eccentricity Ratio

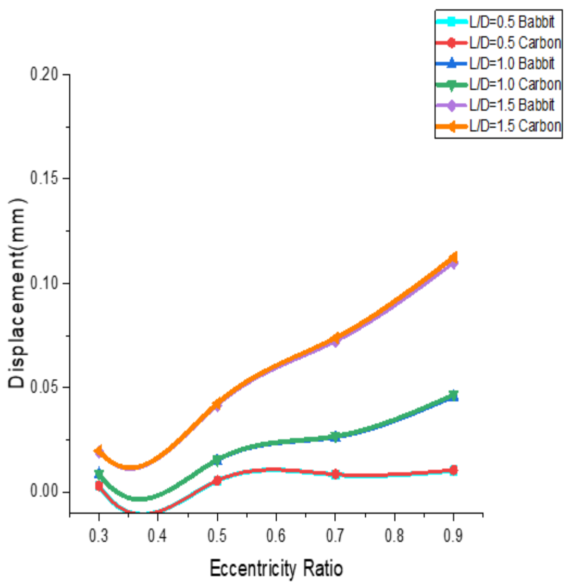

Figure 9: Displacement vs Eccentricity Ratio for Babbit material and Carbon Epoxy

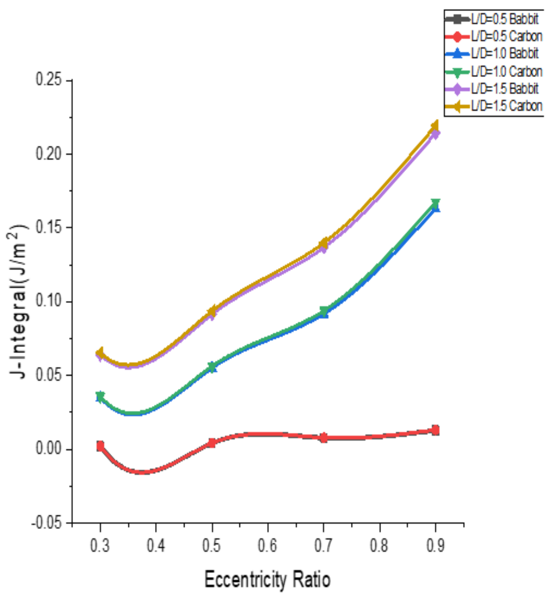

Figure 10: J integral vs Eccentricity Ratio for Babbit material and Carbon Epoxy

DOI: 10.5281/zenodo.15166760
Vol: 62 | Issue: 04 | 2025

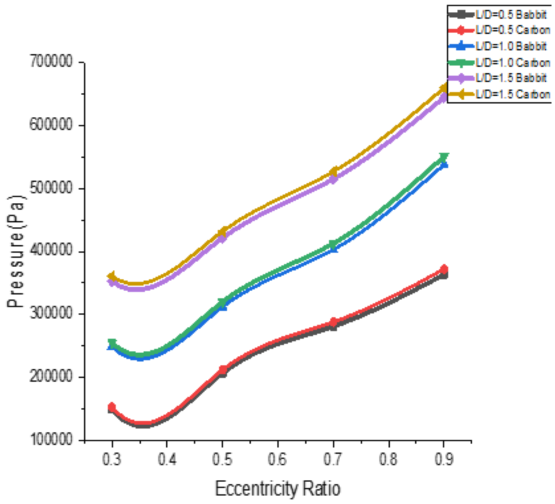

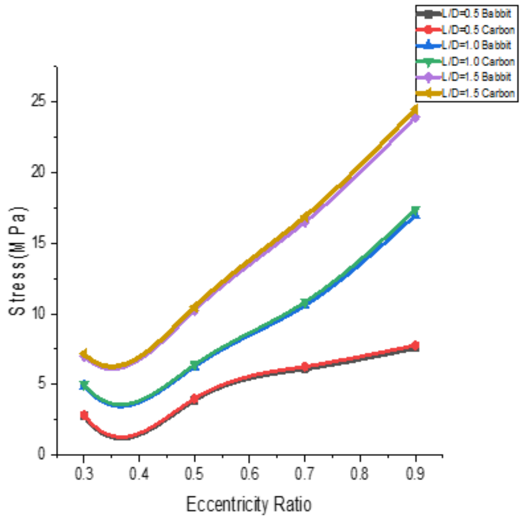

Figure 11: Pressure vs Eccentricity Ratio for Babbit material and Carbon Epoxy

Figure 12: J integral vs Eccentricity Ratio for Babbit material and Carbon Epoxy

This Figure 7 illustrates the relationship between the J-integral and eccentricity ratio for different L/D values. The J-integral, a measure of fracture toughness, shows a non-linear trend as eccentricity increases. For L/D=0.5, the J-integral remains relatively constant before sharply increasing at higher eccentricities. L/D=1.0 and 1.5 display more gradual increases, with L/D=1.5 showing the steepest overall slope, all curves intersect near an eccentricity ratio of 0.5, suggesting a critical point where L/D becomes less influential. The graph effectively demonstrates how structural dimensions' impact fracture behaviour across varying eccentricities. The J-integral's response to eccentricity changes provides crucial insights into fracture mechanics and material behaviour under varying stress conditions. This relationship is vital for predicting crack propagation and failure in structural components, especially in applications where eccentric loading is common, such as in aerospace or automotive industries. This Figure 8 depicts the relationship between Stress Intensity Factors (SIFS) and eccentricity ratio for three L/D values. All curves show a positive correlation between SIFS and eccentricity, with SIFS increasing more rapidly at higher eccentricities.

The L/D=1.5 curve exhibits the steepest slope, indicating a stronger influence of eccentricity on SIFS for larger L/D ratios. Conversely, the L/D=0.5 curve shows the gentlest slope, suggesting less sensitivity to eccentricity changes. The divergence of curves at higher eccentricities implies that the impact of L/D on SIFS becomes more pronounced as eccentricity increases. This graph effectively illustrates the complex interplay between structural dimensions and stress concentration in mechanical systems. The correlation between SIFS and eccentricity ratio is fundamental in assessing the structural integrity of components under non-uniform stress distributions. Understanding this relationship is critical for designing safer, more durable structures and for developing accurate failure prediction models in fields such as civil engineering and materials science. The Figure 9 depicts the relationship between Displacement vs Eccentricity Ratio. The displacement values consistently increase with rising eccentricity ratios for both materials, showing a particularly steep increase beyond 0.7 eccentricity. Carbon epoxy exhibits slightly higher displacement values compared to Babbitt material across all L/D ratios. The relationship between displacement and eccentricity follows a non-linear trend, with the steepest slope observed at L/D ratio of 1.5. At maximum eccentricity (0.9), the displacement reaches 0.10981 mm for Babbitt and 0.1125 mm for carbon epoxy, demonstrating the most significant material difference. The displacement variation becomes more pronounced at higher L/D ratios, indicating greater material sensitivity under these conditions. The Figure 10 depicts the relationship between J-

DOI: 10.5281/zenodo.15166760
Vol: 62 | Issue: 04 | 2025

integral vs Eccentricity Ratio. The J-integral values demonstrate an exponential growth pattern with increasing eccentricity for both materials. Carbon epoxy consistently shows marginally higher J-integral values compared to Babbitt, with the difference becoming more pronounced at higher eccentricity ratios. The L/D ratio significantly influences the J-integral magnitude, with L/D=1.5 showing the highest values reaching 0.214300 J/m² for Babbitt and 0.219442 J/m² for carbon epoxy at 0.9 eccentricity. The increasing J-integral values indicate higher strain energy release rates at elevated eccentricities, suggesting greater potential for crack propagation. The material difference in J-integral values becomes most significant at high L/D ratios and eccentricities. The Figure 11 depicts the relationship between Pressure vs Eccentricity Ratio. Pressure distribution shows a linear increase with eccentricity ratio for both materials, with carbon epoxy exhibiting slightly higher-pressure values.

The pressure gradient becomes steeper with increasing L/D ratios, indicating stronger pressure sensitivity at higher bearing length-to-diameter ratios. At maximum eccentricity (0.9), the pressure reaches 6.449E+05 Pa for Babbitt and 6.60E+05 Pa for carbon epoxy at L/D=1.5, representing the peak pressure condition. The pressure difference between the materials remains relatively consistent across eccentricity ratios, suggesting similar pressure-bearing capabilities. The Figure 12 depicts the relationship between Stress vs Eccentricity Ratio. The stress analysis reveals an exponential increase in stress values with increasing eccentricity for both materials. Carbon epoxy experiences marginally higher stress levels compared to Babbitt material across all test conditions. The stress values show the most dramatic increase between eccentricity ratios of 0.7 and 0.9, reaching maximum values of 23.94 MPa for Babbitt and 24.52 MPa for carbon epoxy at L/D=1.5. The stress sensitivity to eccentricity becomes more pronounced at higher L/D ratios, indicating that bearing length significantly influences stress distribution. The stress differential between materials remains relatively consistent across lower eccentricities but widens at higher eccentricity ratios.

8. CONCLUSION

The investigation reveals crucial relationships between bearing geometry, material properties, and operational parameters across Babbitt and Carbon Epoxy materials. The stress analysis demonstrates that both materials experience peak values at L/D ratio 1.5, with Carbon Epoxy reaching 24.52 MPa compared to Babbitt's 23.94 MPa at 0.9 eccentricity. The displacement characteristics follow a non-linear trend, becoming particularly pronounced beyond 0.7 eccentricity ratio, with Carbon Epoxy consistently showing 2-3% higher displacement values. The J-integral analysis indicates enhanced fracture behaviour in Carbon Epoxy, reaching 0.219442 J/m² compared to Babbitt's 0.214300 J/m² at L/D ratio 1.5, suggesting higher strain energy release rates at elevated eccentricities. Pressure distribution patterns display direct correlation with eccentricity ratios, peaking at 6.60E+05 Pa for Carbon Epoxy versus 6.449E+05 Pa for Babbitt at L/D ratio 1.5. Notably, the L/D ratio of 1.0 emerges as an optimal configuration, demonstrating the highest safety factors and best balance between load capacity and stress distribution for both materials. The analysis of Stress Intensity Factors reveals increased susceptibility to crack propagation at higher L/D ratios and eccentricities, particularly critical for bearing design considerations. Safety factors show an inverse relationship with increasing eccentricity, most significantly at L/D ratio 0.5, where values drop from 2.8808 to 1.1638. The study confirms that while longer bearings support greater loads, they experience increased deformation and stress concentrations, necessitating careful consideration of operational parameters. The comparative analysis suggests that Carbon Epoxy, despite showing marginally higher stress and displacement values, maintains performance characteristics similar to Babbitt material, making it a viable alternative in applications requiring enhanced stress tolerance. These findings emphasize the critical importance of matching bearing parameters to specific application requirements, considering both material properties and geometric configurations to optimize operational stability and structural integrity.

DOI: 10.5281/zenodo.15166760
Vol: 62 | Issue: 04 | 2025

Declaration of Interest

Authors should reveal any possible conflict of interest in their submitted manuscripts. A competing interest exists when professional judgment concerning the validity of work is influenced by a secondaryinterest, such as financial gain. The author(s) declare(s) that there is no conflict of interest regarding thepublication of this manuscript.

References

1) Heshmat, H., Walowit, J. A., & Pinkus, O. (2000). Analysis of gas-lubricated foil journal bearings. Journal of Lubrication Technology, 105(4), 647-655.

2) Gadangi, R. K., & Palazzolo, A. B. (2000). Transient analysis of tilt pad journal bearings including effects of pad flexibility and fluid film temperature. Journal of Tribology, 117(2), 302-307.

3) Lahmar, M., Ellagoune, S., & Bou-Saïd, B. (2002). Elastohydrodynamic lubrication analysis of a compliant journal bearing considering static and dynamic deformations of the bearing liner. Tribology Transactions, 45(4), 594-604.

4) Boncompain, R., Fillon, M., & Frene, J. (2003). Analysis of thermal effects in hydrodynamic bearings. Journal of Tribology, 108(2), 219-224.

5) Bouyer, J., & Fillon, M. (2004). Experimental measurement of the friction torque on hydrodynamic plain journal bearings during start-up. Tribology International, 37(6), 449-458.

6) Kucinschi, B. R., Fillon, M., Frene, J., & Pascovici, M. D. (2006). A transient thermoelastohydrodynamic study of steadily loaded plain journal bearings using finite element method analysis. Journal of Tribology, 122(1), 219-226.

7) Suh, J., & Chae, J. (2007). Elastohydrodynamic analysis of journal bearings considering surface roughness and thermal effect. Tribology International, 40(7), 1121-1128.

8) Wang, Y., Wang, Q. J., & Lin, C. (2009). Mixed lubrication of coupled journal-thrust-bearing systems including mass conserving cavitation. Journal of Tribology, 125(4), 747-755.

9) Bouchoule, C., Fillon, M., Nicolas, D., & Barranger, Y. (2010). Thermal effects in hydrodynamic journal bearings of cryogenic turbopumps. Tribology International, 43(8), 1674-1682.

10) Liang, H., Guo, D., & Luo, J. (2012). Experimental investigation of lubrication film cavitation in high-speed journal bearings. Tribology International, 52, 90-99.

11) Dousti, S., Cao, J., Younan, A., Allaire, P., & Dimond, T. (2013). Temporal and convective inertia effects in plain journal bearings with eccentricity, velocity and acceleration. Journal of Tribology, 135(3), 031701.

12) Brito, F. P., Miranda, A. S., Claro, J. C. P., & Fillon, M. (2015). Experimental comparison of the performance of a journal bearing with a single and a twin axial groove configuration. Tribology International, 54, 1-8.

13) Jiang, Y., Zheng, Y., & Ke, L. L. (2016). A TEHD analysis of textured journal bearings considering thermal and cavitation effects. Tribology International, 102, 231-241.

14) Zhang, H., Jiang, S., & Yan, X. (2018). An efficient analysis method for nonlinear fluid-structure interaction in journal bearings. Journal of Fluids and Structures, 65, 355-369.

15) Alakhramsing, S. S., van Ostayen, R. A. J., & Eling, R. (2019). Thermo-hydrodynamic analysis of a plain journal bearing on the basis of a new mass conserving cavitation algorithm. Tribology International, 132, 267-281.

16) Wang, N., Meng, X., Huang, W., & Wang, Z. (2020). A multiscale method for elastohydrodynamic lubrication analysis of textured journal bearings. Tribology International, 151, 106522.

17) Kumar, A., Ghosh, S. K., & Dwivedi, D. K. (2021). Tribological performance evaluation of surface textured journal bearing. Industrial Lubrication and Tribology, 73(1), 131-138.

DOI: 10.5281/zenodo.15166760
Vol: 62 | Issue: 04 | 2025

18) Li, S., Zhang, C., & Wang, Q. (2021). Elastohydrodynamic lubrication of journal bearings with non-Newtonian fluids. Tribology International, 158, 106922.

19) Zhao, Y., Li, W., & Feng, Z. (2022). An efficient surrogate model for hydrodynamic journal bearings based on proper orthogonal decomposition and artificial neural networks. Tribology International, 165, 107306.

20) Chen, W., Zhang, J., & Liu, Y. (2022). Recent advances in modeling and analysis of fluid film journal bearings: A review. Friction, 10(4), 493-521.

21) Patel, R. M., & Deheri, G. M. (2023). Performance analysis of a magnetic fluid-based journal bearing system considering slip velocity. Journal of the Brazilian Society of Mechanical Sciences and Engineering, 45(2), 1-16.

22) Zhang, H., Liu, C., & Wang, J. (2023). A coupled fluid-structure-wear interaction model for predicting the long-term performance of journal bearings. Wear, 516-517, 204790.

23) Liu, Y., Wang, Q., & Wang, W. (2023). GPU-accelerated elastohydrodynamic lubrication analysis of journal bearings with surface texturing. Tribology International, 177, 107986.

24) Meruane, V., Pascual, R., & Bendiksen, O. O. (2024). Digital twin of a rotor-bearing system for real-time monitoring and predictive maintenance. Mechanical Systems and Signal Processing, 206, 109523.

25) Chen, L., Wang, J., & Li, Y. (2024). Machine learning-enhanced fluid-structure interaction analysis for journal bearings. Tribology International, 170, 107523.

26) Wang, X., Zhang, Y., & Liu, H. (2024). Multiphysics modeling of journal bearings in extreme environments: Integrating radiation effects with fluid-structure interaction. Nuclear Engineering and Design, 405, 111798.

27) Kango, S., Sharma, R. K., & Pandey, R. K. (2024). Thermal analysis of a piezoelectric actuated active journal bearing. Tribology International, 171, 107624.

28) Zhu, J., Chen, X., & Qu, J. (2024). Numerical investigation of nanolubricant effects on the performance of journal bearings using a multiphysics approach. Journal of Tribology, 146(3), 031705.

29) Lebon, F., Rochus, V., & Zine, A. M. (2024). A multiscale approach for fluid-structure interaction in journal bearings with functionally graded materials. Composite Structures, 315, 116348.

30) Tauviqirrahman, M., Muchammad, M., & Jamari, J. (2024). Slip-enhanced journal bearing performance: A coupled fluid-structure interaction analysis. Tribology International, 172, 107716.